An Approximate Inverse to the Extended Born Modeling Operator

Jie Hou, William W. Symes, The Rice Inversion Project, Rice University

SUMMARY

We modify RTM to create an approximate inverse to the extended Born modeling operator in 2D. The derivation uses asymptotic ray theory and stationary phase principle, but the result applies directly to RTM. The inverse operator differs from the adjoint operator only by application of several explicit velocity-independent filters. This inverse operator, on the one hand, can be used as true amplitude migration (in the asymptotic sense). On the other hand, it can be used as preconditioner to speed up the iterations of Least-Squares Migration and Full Waveform Inversion.

INTRODUCTION

Seismic imaging is a process of converting seismic reflection data into subsurface image based on a given background velocity model. This process is usually accomplished by migration, which can position reflectors correctly but with generally incorrect amplitudes and phases. In fact, various migration algorithms compute the adjoint of the Born (linearized) forward modeling operator, or an approximation to it, rather than an approximate inverse. In this paper, we show how to inexpensively modify Reverse Time Migration (RTM) to produce an approximate inverse.

The investigation of the inverse Born operator started with the development of generalized Radon transform (GRT) inversion to compensate for the amplitude loss of geometric spreading in Kirchhoff Migration (Beylkin (1985), Bleistein (1987),Schleicher et al. (1993), Tygel et al. (1997)). GRT inversion applies a weight function to the seismic data before the diffraction stack. This method has been widely used due to its simplicity and efficiency. However, because of its ray-based nature, it may produce a poor quality image in complex geological settings. Wave-equation true amplitude migration based on one-way equation (Zhang et al. (2003, 2005)) provides better images in complex overburden, but suffers from propagation angle limitation. Zhang et al. (2007), Zhang and Sun (2009) show a modification of the boundary conditions used in the wave equation combined with a proper imaging condition can lead to a true amplitude RTM accurate at all angles. The algorithm described here is closely related to that of Zhang and Sun (2009), but does not require the modification of the standard imaging condition.

Iterative inversion of the Born or linearized scattering operator has become known as least squares migration (LSM), see Tarantola (1984), LeBras and Clayton (1988), Bourgeois et al. (1989), Lambare et al. (1992), Nemeth et al. (1999), Kühl and Sacchi (2003), Tang (2009). Iterative inversion permits straightforward modification of problem definition, for example by inclusion of regularization or target-oriented restriction, but is relatively expensive. Tens of iterations are generally needed for a good result, each costing as much as two migrations.

The present work was inspired by ten Kroode (2012), whose construction amounts to a true-amplitude modification of Claerbout's survey sinking imaging principle (Claerbout (1985)), in 3D. Survey-sinking migration amounts to the adjoint of an extended modeling operator, which operates on nonphysical models depending on both spatial coordinates and subsurface offset parameters (Stolk and De Hoop (2006); Symes (2008); Stolk et al. (2009b)). We develop a modification of ten Kroode's approximate inverse in 2D and provide numerical examples to illustrate its effectiveness. In the concluding section, we mention the applicability of this operator to ordinary (non-extended) Born inversion, and to acceleration of LSM iteration.

THEORY

In this section, we will first review the concepts of the extended Born modeling operator, its adjoint operator and their high frequency approximations. We will then derive and implement an approximate inverse operator.

Extended Born Modeling Operator and its Adjoint

The Constant Density Acoustic Wave Equation is :

$$\frac{1}{v^2(\mathbf{x})}\frac{\partial^2 u}{\partial t^2}(\mathbf{x},t) - \nabla^2 u(\mathbf{x},t) = f(t,\mathbf{x},\mathbf{x_s}) \tag{1}$$

Here $\mathbf{x}$ denotes position within a model of the Earth, $v(\mathbf{x})$ is the acoustic velocity, $u(\mathbf{x_s},\mathbf{x},t)$ is the acoustic potential, and $f(t,\mathbf{x},\mathbf{x_s})$ is the source term. We assume throughout this paper that v is constant in the half-space $z < 0$, that is, that $z = 0$ is an absorbing surface.

The Born (linearized, single scattering) approximation splits the coefficient v into a smooth or long-scale background model v_0, and a short- or wavelength-scale perturbation δv : $v(\mathbf{x}) = v_0(\mathbf{x}) + \delta v(\mathbf{x})$. The first order perturbation in the acoustic potential field δu corresponding to δv may be expressed in terms of the causal Green's function $G(\mathbf{x},\mathbf{y},t)$ for background model v_0. Restricting δu to the source and receiver positions $\mathbf{x_s},\mathbf{x_r}$ results in an integral operator expression for the Born modeling operator $F[v_0]$:

$$\begin{aligned} &F[v_0]\delta v(\mathbf{x_s},\mathbf{x_r},t) \\ &= \frac{\partial^2}{\partial t^2}\int d\mathbf{x}d\tau G(\mathbf{x_s},\mathbf{x},\tau)\frac{2\delta v(\mathbf{x})}{v_0(\mathbf{x})^3}G(\mathbf{x},\mathbf{x_r},t-\tau) \end{aligned} \tag{2}$$

The adjoint operator $F[v_0]^*$ is the operator implemented by one common variant of Reverse Time Migration. The scale conditions on $v_0, \delta v$ are sufficient to make δu a good approximation to the actual perturbation in the acoustic field resulting from δv.

An appropriate version of subsurface offset extended Born modeling introduces dependence of δv (but not v_0) on an additional parameter, $\mathbf{h}$, essentially the offset between sunken source and sunken receiver in Claerbout's survey-sinking imaging condition (Claerbout (1985), Symes (2008), Stolk et al. (2009b)). In terms of Green's functions, the subsurface extended Born Modeling Operator and its adjoint (applied to a data perturbation δd) are :

$$\begin{aligned}&\bar{F}[v_0]\delta v(\mathbf{x_s},\mathbf{x_r},t)\\&=\frac{\partial^2}{\partial t^2}\int d\mathbf{x}d\mathbf{h}d\tau G(\mathbf{x_s},\mathbf{x}-\mathbf{h},\tau)\frac{2\delta v(\mathbf{x},\mathbf{h})}{v_0(\mathbf{x})^3}G(\mathbf{x}+\mathbf{h},\mathbf{x_r},t-\tau)\end{aligned} \tag{3}$$

$$\begin{aligned}&\bar{F}^*[v_0]\delta d(\mathbf{x},\mathbf{h})\\&=-\frac{2}{v_0(\mathbf{x})^3}\int d\mathbf{x_s}d\mathbf{x_r}dtd\tau G(\mathbf{x_s},\mathbf{x}-\mathbf{h},\tau)G(\mathbf{x}+\mathbf{h},\mathbf{x_r},t-\tau)\\&\times\frac{\partial^2}{\partial t^2}\delta d(\mathbf{x_s},\mathbf{x_r},t)\end{aligned} \tag{4}$$

In Claerbout's original conception, the subsurface offset $\mathbf{h}$ is horizontal. ten Kroode also adopts this convention, and we follow it here. Thus we write h rather than $\mathbf{h}$ for the (scalar) horizontal subsurface offset in 2D.

High Frequency Approximation

Both to understand the high frequency leading order behaviour of the normal operator or Hessian $\bar{F}^*[v_0]\bar{F}[v_0]$, and to see how to modify $\bar{F}^*$ so that the normal operator becomes an approximate identity, we introduce the progressing wave approximation (Courant and Hilbert (1966)) of the Green's function: with a suitable choice of singular, causal waveform $S(t)$,

$$G(\mathbf{x_s},\mathbf{x},t)\cong a(\mathbf{x_s},\mathbf{x})S(t-\tau(\mathbf{x_s},\mathbf{x})) \tag{5}$$

In equation (5), the amplitude $a(\mathbf{x_s},\mathbf{x})$ and the travel time $\tau(\mathbf{x_s},\mathbf{x})$ solve the transport and eikonal equation respectively. The approximation (5) is only valid locally, between the source point and the nearest caustic or conjugate (multipath) point. The conclusions we draw below are valid more globally, however, provided that the Traveltime Injectivity Condition holds: a two-way traveltime along a reflected ray pair determines the one-way traveltimes of source and receiver rays. ten Kroode (2012) gives a detailed justification for the global validity of similar conclusions in the 3D case. We confine ourselves in this paper to numerical evidence for global 2D results.

In 2D case, the leading singularity is proportional to the generalized function $S(t)=t_+^{-1/2}=t^{-1/2}H(t)$. Replacing the Green's function by the progressing wave approximation (5) in the expression (3) for the extended Born modeling operator and using the identity (Gel'fand and Shilov (1958)),

$$t_+^{-1/2}*t_+^{-1/2}=(\Gamma(\frac{1}{2}))^2H(t)=\pi H(t) \tag{6}$$

we obtain

$$\bar{F}[v_0]\delta v(\mathbf{x_s},\mathbf{x_r},t)\cong\frac{\partial}{\partial t}\int d\mathbf{x}dha_sa_r\delta(t-T_s-T_r)\frac{2\pi\delta v(\mathbf{x},h)}{v_0(\mathbf{x})^3} \tag{7}$$

in which we have denoted amplitudes $a(\mathbf{x_s},\mathbf{x}-h),a(\mathbf{x}+h,\mathbf{x_r})$ as a_s,a_r and traveltime $\tau(\mathbf{x_s},\mathbf{x}-h),\tau(\mathbf{x}+h,\mathbf{x_r})$ as T_s,T_r. We can also give the same treatment to the migration operator :

$$\bar{F}[v_0]^*\delta d(\mathbf{x},h)\cong-\frac{2\pi}{v_0(\mathbf{x})^3}\int d\mathbf{x_s}d\mathbf{x_r}a_sa_r\frac{\partial}{\partial t}\delta d(\mathbf{x_s},\mathbf{x_r},T_s+T_r) \tag{8}$$

Combining equations (3) and (4) yields a five-fold integral involving two copies of the extended space variables $(\mathbf{x},h)$ as well as integration over the acquisition coordinates. For idealized 2D acquisition, the source and receiver locations lie along a horizontal lines at depths z_s,z_r, so the acquisition coordinates may be chosen as x_s,x_r. An asymptotic evaluation of this integral follows along the lines of Beylkin (1985); Symes (1998), with a novel twist. One accounts for the delta function $\delta(t-T_r-T_s)$ in equation (3) by writing z as a function of x,h,t,x_s,x_r, assuming that reflectors are subhorizontal (if not, then a vertical offset extension is required). One then introduces the Fourier transform of $\delta v(x,z,h)$, and uses the principle of stationary phase to evaluate the multiple integral for large wavenumber. The integrations are naturally paired as (x,x_r) and (h,x_s). Each pair of integrals gives rise to a Hessian determinant factor. These *Beylkin determinants* are actually proportional to reciprocal amplitudes (Zhang et al. (2005)). The non-extended asymptotic computation includes the integration over (x,x_r) and cancels the receiver amplitude a_r, however the remaining geometric amplitude a_s must be removed via an appropriate imaging condition (Stolk et al. (2009a)). The extended computation, however, involves the additional integration over (h,x_s), producing an additional Beylkin determinant which cancels a_s.

The upshot is that no ray-theoretic quantities remain in the normal operator, merely several velocity-independent filters and scaling by a power of the velocity. Compensation for these leads to the expression for an approximate inverse:

$$\bar{F}^{-1}[v_0]\delta d(\mathbf{x},h)=-8|kk'|v_0^6\bar{F}^*[v]I_t^4D_{z_s}D_{z_r}\delta d(\mathbf{x},h) \tag{9}$$

where $k=(k_x,k_z)$ and $k'=(k_h,k_z)$ are the wavenumbers (acting as filters, and easily applied via Fourier transform), I_t is the time integral and D_{z_s},D_{z_r} are the source and receiver depth derivative. For the baseline examples below, we set $z_s=z_r=0$, explicitly computed data for sources and receivers at $\pm\Delta z_s,\pm\Delta z_r$, and formed centered differences. We will address this point in the discussion below.

NUMERICAL EXAMPLES

In this section, we will use two numerical examples to illustrate the effectiveness of the inverse operator.

The first model combines a single flat reflector at $z=1.5$ km, with Gaussian derivative wavelet, with a constant (2500 m/s) background velocity. The spatial sampling interval of the model is 20m for both x and z axis. A (2.5-5-30-35) Hz bandpass wavelet with 2ms time interval is used to simulate the Born data (2-8 Finite Difference Scheme). 31 shots are evenly spread on the surface ($z=0$) every 100m. All the shots will be recorded by 301 receivers deployed every 10m on the surface.

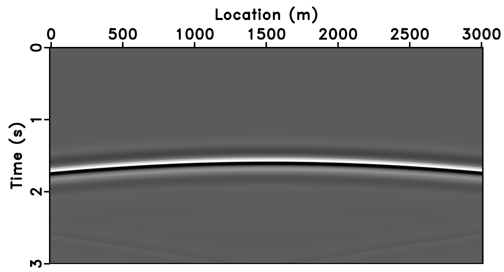

(a)

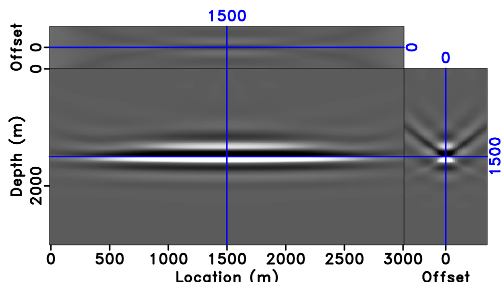

(b)

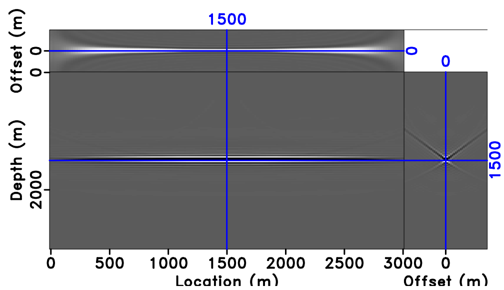

(c)

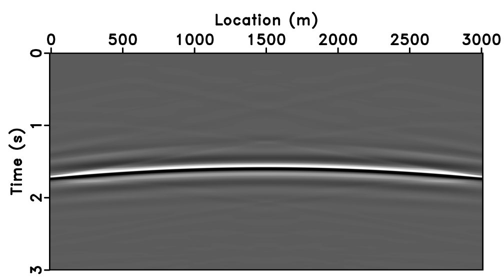

(d)

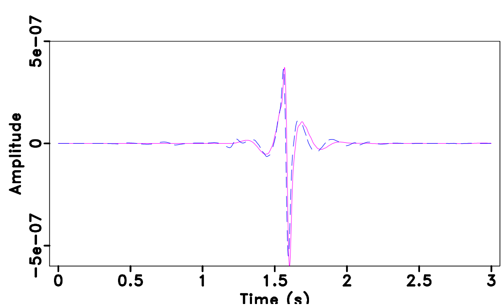

(e)

Figure 1: (a) One-shot ($x_s = 1500m$) Simulated Born Data (b) Extended RTM image (c) Inverted Image (d) Resimulated Data of the Inverted Image (e) One trace comparison ($x = 1500m$) between the observed data (red solid line) and predicted data from inverted image (blue dashed line)

The Born data shown in Figure 1(a) is calculated using Equation (3). Both extended RTM (equation (4)) and the new inverse operator (Equation (9)) are applied on the Born data. Comparing the migrated image (Figure 1(b)) and inverted image (Figure 1(c)), we can clearly see the inverse operator can focus the energy much better than extended RTM. The inverse operator can recover both kinematic and dynamic information from the reflection data. The reflector recovered by the inverse operator is then very close to the true reflectivity model. However, we can never recover the reflector perfectly due to the lack of the low frequency data. A good way to evaluate the inverse operator would be to compare the “observed” data of the true model (Figure 1(a)) and the “predicted” data of inverted image (Figures 1(d), 1(e)). The comparisons show that the data predicted from the inverted model is almost same as the “observed” data.

The simple geometrical optics computation of previous section will fail in the presence of caustics (or multipathing). The background velocity model for the second example contains a low velocity Gaussian lens. A flat horizontal reflector (same as the one in the first example) is placed right below the lens at the depth of 2km. This model is very similar to the one used by Nolan and Symes (1996) and Stolk and Symes (2004). The numerical implementation has the same configuration as the first example. Because of the Gaussian lens, the rays will certainly focus and form the triplication after going through the lens. The rays and wavefronts are shown in Figure 2(b). We can clearly see that this model produces multipathing and caustics.

The inverse operator defined in equation (9) produces the reflectivity model shown in Figure 3(b). From the image perspective, we clearly reproduce the flat reflector below the lens with no kinematic artifacts (Stolk and Symes (2004)). Resimulation with Born modeling operator from the inverted reflectivity model predicts data very close to the input data (Figures 3(c), Figure 3(d)).

CONCLUSION

A simple modification of subsurface offset extended RTM produces an asymptotic inverse to the Born scattering operator. Implementation of straightforward, and numerical experiments suggest that within its domain of applicability, this inversion operator is quite accurate.

On its face, the inverse operator approximately inverts the extended Born modeling operator, therefore may be used to accelerate convergence of the reflectivity estimation loop in automated velocity model building (for example, Liu et al. (2013)). However it may also be used as an approximate inverse to ordinary Born modeling, hence to accelerate iterative LSM, simply via post-application of any inverse to the extension operator. Apparently, simple stacking of the extended inversion is sufficient in some cases.

ten Kroode (2012) suggests that the necessary D_{z_s}, D_{z_r} operators may be applied to the data via one-way approximation. Alternatively, the authors have observed that for streamer data

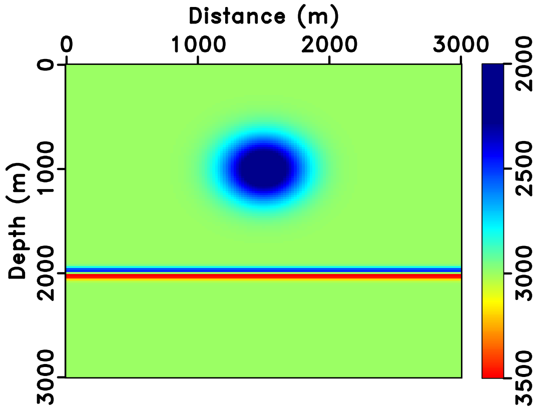

(a)

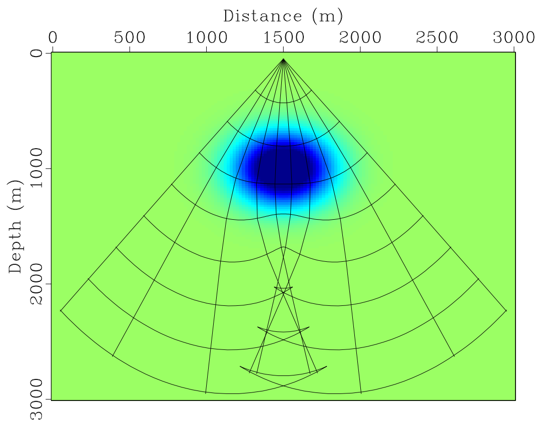

(b)

Figure 2: (a) Gaussian lens background velocity model with a reflector at 2km (b) The rays and wavefronts in the Gaussian lens velocity model

with shallow tow depths, the ghost sources and receivers automatically supply scaled versions of these derivatives. That is, only the remaining filters in equation (9) need be applied, in conjunction with the absorbing surface RTM.

ACKNOWLEDGMENTS

We are grateful to the sponsors of The Rice Inversion Project (TRIP) for their long-term support, and to Fons ten Kroode for inspiring our work. The first author would like to thank Yujin Liu for providing the prototype code for extended RTM.

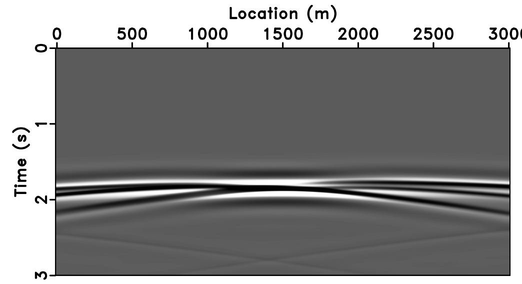

(a)

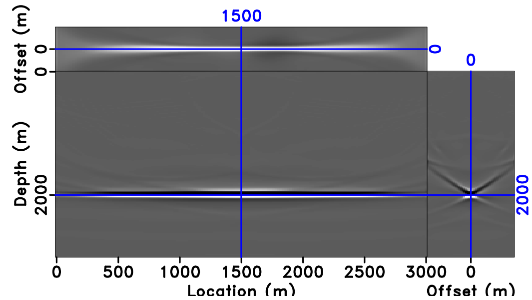

(b)

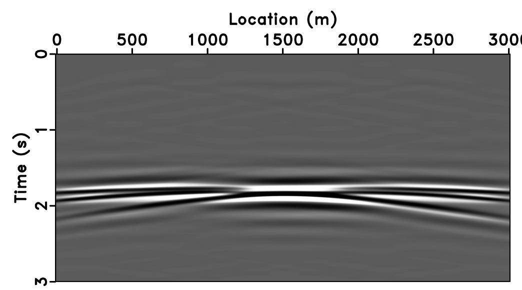

(c)

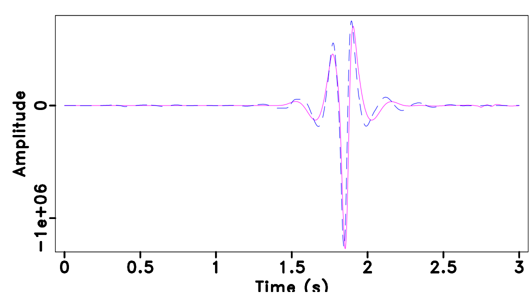

(d)

Figure 3: (a) One-shot ($x_s = 1500m$) Simulated Born Data of the velocity model shown in Figure 2(a) (b) Inverted image using the new inverse operator (c) Resimulated data of the inverted image (d) One trace comparison (x=1500m) of the data shown in (a) (red solid line) and (c) (blue dashed line)

REFERENCES

Beylkin, G., 1985, Imaging of discontinuities in the inverse scattering problem by inversion of a causal generalized Radon transform: Journal of Mathematical Physics, **26**, 99–108.

Bleistein, N., 1987, On the imaging of reflectors in the earth: Geophysics, **52**, 931–942.

Bourgeois, A., B. Jiang, and P. Lailly, 1989, Linearized inversion: A significant step beyond pre-stack migration: Geophysical Journal International, **99**, 435–445.

Claerbout, J. F., 1985, Imaging the earth's interior: Blackwell Scientific Publishers.

Courant, R., and D. Hilbert, 1966, Methods of mathematical physics: CUP Archive, **1**.

Gel'fand, I., and G. Shilov, 1958, Generalized Functions: volume 1: Academic Press.

Kühl, H., and M. D. Sacchi, 2003, Least-squares wave-equation migration for AVO/AVA inversion: Geophysics, **68**, 262–273.

Lambare, G., J. Virieux, R. Madariaga, and S. Jin, 1992, Iterative asymptotic inversion in the acoustic approximation: Geophysics, **57**, 1138–1154.

LeBras, R., and R. W. Clayton, 1988, An iterative inversion of back-scattered acoustic waves: Geophysics, **53**, 501–508.

Liu, Y., W. W. Symes, Y. Huang, and Z. Li, 2013, Inversion velocity analysis via differential semblance optimization in the depth oriented extension: Presented at the 83rdth Annual International Meeting, Expanded Abstracts, Society of Exploration Geophysicists.

Nemeth, T., C. Wu, and G. T. Schuster, 1999, Least-squares migration of incomplete reflection data: Geophysics, **64**, 208–221.

Nolan, C. J., and W. W. Symes, 1996, Imaging and coherency in complex structures: 66th Annual International Meeting, Expanded Abstracts, Society of Exploration Geophysicists, 359–363.

Schleicher, J., M. Tygel, and P. Hubral, 1993, 3-D true-amplitude finite-offset migration: Geophysics, **58**, 1112–1126.

Stolk, C. C., and M. V. De Hoop, 2006, Seismic inverse scattering in the downward continuation approach: Wave Motion, **43**, 579–598.

Stolk, C. C., M. V. de Hoop, and T. P. M. Op 't Root, 2009a, Reverse time migration inversion from single-shot data: Presented at the 79th Annual International Meeting, Expanded Abstracts, Society of Exploration Geophysicists.

Stolk, C. C., M. V. de Hoop, and W. W. Symes, 2009b, Kinematics of shot-geophone migration: Geophysics, **74**, WCA18–WCA34.

Stolk, C. C., and W. W. Symes, 2004, Kinematic artifacts in prestack depth migration: Geophysics, **69**, 562–575.

Symes, W. W., 1998, Mathematics of reflection seismology. (available at http://www.trip.caam.rice.edu).

———, 2008, Migration velocity analysis and waveform inversion: Geophysical Prospecting, **56**, 765–790.

Tang, Y., 2009, Target-oriented wave-equation least-squares migration/inversion with phase-encoded hessian: Geophysics, **74**, WCA95–WCA107.

Tarantola, A., 1984, Linearized inversion of seismic reflection data: Geophysical prospecting, **32**, 998–1015.

ten Kroode, F., 2012, A wave-equation-based Kirchhoff operator: Inverse Problems, **28**, 115013:1–28.

Tygel, M., J. Schleicher, P. Hubral, and L. T. Santos, 1997, 2.5-d true-amplitude kirchhoff migration to zero offset in laterally inhomogeneous media: Geophysics, **63**, 557–573.

Zhang, Y., and J. Sun, 2009, Practical issues of reverse time migration-true-amplitude gathers, noise removal and harmonic-source encoding: First Break, **27**, 53–59.

Zhang, Y., J. Sun, S. Gray, et al., 2007, Reverse-time migration: amplitude and implementation issues: 77th Annual International Meeting, Expanded Abstracts, Society of Exploration Geophysicists, 2145–2149.

Zhang, Y., G. Zhang, and N. Bleistein, 2003, True amplitude wave equation migration arising from true amplitude one-way wave equations: Inverse Problems, **19**, 1113–1138.

———, 2005, Theory of true-amplitude one-way wave equations and true-amplitude common-shot migration: Geophysics, **70**, E1–E10.